ELSEVIER

Polymer 41 (2000) 1409–1428

polymer

Fractionated crystallization in immiscible POM/(PS/PPE) blends Part 1: effect of blend phase morphology and physical state of the amorphous matrix phase

V. Everaert[a], G. Groeninckx[a,*], L. Aerts[b]

[a]*Catholic University of Leuven, Department of Chemistry, Laboratory for Macromolecular Structural Chemistry, Celestijnenlaan 200F, B-3001 Heverlee, Belgium*

[b]*Dow Benelux N.V., P.O. Box 48, 4530 AA Terneuzen, The Netherlands*

Abstract

The fractionated crystallization behavior of POM in immiscible POM/(PS/PPE) blends has been investigated by Differential Scanning Calorimetry (DSC) and correlated to the blend phase morphology. By varying the PS/PPE composition, homogeneous amorphous phases with different glass transition temperatures, varying between 100 ($T_{g,PS}$) and 215°C ($T_{g,PPE}$), and melt-viscosities were obtained, without altering the interfacial tension of the blend system. As such, a model blend system has been created which allows to investigate both the influence of the blend phase morphology and of the physical state of the amorphous PS/PPE matrix, on the crystallization behavior of the minor POM phase.

The difference between low viscosity/low viscosity and low viscosity/high viscosity blend systems with respect to the development of the phase morphology during melt-mixing is reflected in various aspects of the fractionated crystallization behavior. The onset composition of fractionated crystallization can be related to the center of the phase inversion region for all blend systems. Within the same blend type, the extent of homogeneous crystallization can be related to the blend phase morphology (i.e. the number of droplets per volume unit of the dispersed phase). However, comparing different blend types reveals that other factors, such as the physical state of the amorphous matrix phase, also play a role. Further, multiple crystallization peaks were observed and have been related to the width of the particle size distribution of the dispersed POM phase.

Keywords: POM/(PS/PPE) blends; Immiscible blends; Fractionated crystallization

1. Introduction

Binary mixtures of immiscible polymers where one of the components is in excess, usually have a typical droplet-in-matrix phase morphology. The particle size of the dispersed phase in such blends depends on the blend composition, melt-viscosity and elasticity of each phase, and the mixing conditions [1–3]. In the case where the finely dispersed component is capable of crystallization, the blend phase morphology, has been demonstrated by several authors to have a crucial impact on the crystallization behavior of the dispersed phase, due to the typical fractionated crystallization process [4]. This phenomenon has been investigated only for a limited number of immiscible polymer blend systems, i.e. HDPE/POM [5], PVDF/PA-6 [6,7], PVDF/PBT [6,7], PVDF/PA-66 [8], EPDM/PA-6 [9], PS/iPP [10], PS/LDPE [11], PS/LLDPE [12,13], LLDPE/iPP [13], SBR/iPP [14], PS/PEG [15], iPP/PEG [16], and iPP/PA-6 [17,18]. Often, only a qualitative understanding of the fractionated crystallization behavior was presented.

It has become clear that fractionated crystallization can be considered as subsequent steps of primary nucleation, at different degrees of undercooling, ΔT_c, often ending up with a crystallization peak at the homogeneous nucleation temperature, $T_{c,hom}$ [7,10,11,14]. Koutsky et al. [4] proved that the phenomenon of fractionated crystallization is directly related to the size of the dispersed droplets, by following the amount of solidified polymeric droplets, suspended in an inert liquid medium, via optical microscopy. This technique was first used by Vonnegut [19], and is based on the fact that if a bulk sample is subdivided into numerous small droplets, the available heterogeneities are confined to a small portion of the droplets, and the remaining droplets are free to nucleate at rates governed by the molecular characteristics of the sample. Frensch et al. [7] developed the theoretical background of this phenomenon by relating each fraction that crystallizes upon cooling from the melt, to the primary nucleation

* Corresponding author.

0032-3861/00/$ - see front matter
PII: S0032-3861(99)00321-3

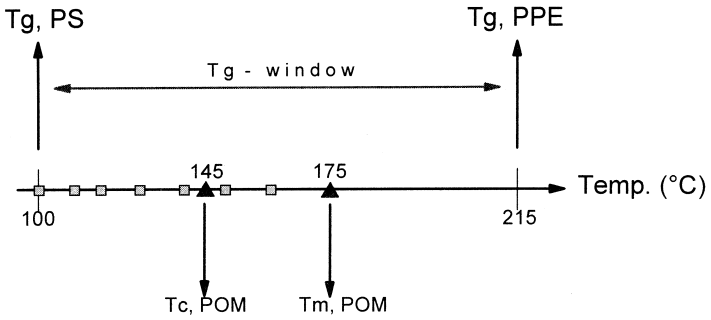

Fig. 1. Schematical representation of the POM/(PS/PPE) model system. The T_g of the amorphous PS/PPE phase can be varied around T_c or T_m of the crystallizable POM phase.

from heterogeneities with a different specific interfacial energy difference, Δy_i, between the polymeric chain and the nucleating substrate. Usually, only those heterogeneities with the smallest Δy-value are efficient in primary nucleation. Via secondary nucleation, the crystallization can spread out over the whole volume and is completed before the undercooling, $\Delta T_{c,2}$, of the heterogeneity with the second smallest Δy-value is reached. However, if the material is dispersed in numerous small volumes, each droplet will start crystallizing from the heterogeneity with the lowest Δy-value in that droplet. As the number of dispersed droplets is often exceeding the number of heterogeneities promoting crystallization around the bulk crystallization temperature, smaller droplets having a lower probability of containing such heterogeneities will show crystallization from other heterogeneities at much higher degrees of undercooling, or even show homogeneous crystallization by the self-association of the polymer chains.

From these theoretical considerations, perspectives could be seen for the prediction of fractionated crystallization in immiscible polymer blends, based on the knowledge of the blend phase morphology and nucleation density of the crystallizable phase, and vice versa. In this paper, fractionated crystallization in immiscible blends of poly(oxymethylene) (POM) dispersed in an amorphous miscible PS/PPE matrix is investigated. This model system allows to vary both the melt-viscosity ratio of the blend system, hence generating different phase morphologies, and the physical state of the amorphous matrix during the crystallization of the dispersed POM droplets (Fig. 1).

An attempt is made to correlate the fractions crystallizing at different degrees of undercooling with the blend phase morphology. The influence of the size of the dispersed phase and the physical state of the amorphous PS/PPE matrix phase is discussed.

2. Experimental

2.1. Materials

The characteristics of the basic materials used in this study are listed in Table 1. POM is a commercial grade Celcon® M-50 POM copolymer (Hoechst Celanese, USA) containing about 5 wt.% ethyleneglycol to stabilize the product against depolymerisation at elevated temperatures. Its melting point is 175°C. Atactic polystyrene (PS) is a commercial grade Styron® E680 (Dow Benelux N.V., Terneuzen, NL). Poly (2,6-dimethyl-1,4-phenylene ether) (PPE) is a PPE-800 grade supplied by General Electric Plastics (Bergen-op-Zoom, NL).

2.2. Miscible amorphous PS/PPE phases

The amorphous phases were prepared by melt-blending PS ($T_g = 102$°C) with PPE ($T_g = 215$°C); both components are perfectly miscible over the whole composition range [20,21]. Changing the blend composition allows to vary both the melt-viscosity and the glass-transition temperature, T_g, of the amorphous PS/PPE phase without altering the interfacial tension between POM and these miscible amorphous components [22]. Blending has been performed on a Haake Rheocord 90 twin screw extruder at 285°C with a screw speed of 120 rpm, after drying the materials for at least one night under vacuum. The homogeneity of each blend was checked by DSC measurements. Table 2 presents

Table 1
Basic material characteristics

Material	MFI (g/10 min)	M_n (GPC)	M_w (GPC)	Polydispersity	Density (g/cm^3)
POM	–		± 70 000		1.4
PS	–	81 900	190 000[a]	2.6	1.055
PPE	13(300°C)	19 300	54 300[a]	2.8	1.065

[a] Measured in THF at 25°C; molecular weights are based on polystyrene standards.

Table 2
Characteristics of the misicible amorphous PS/PPE phases

Blend composition	Code name	T_g (DSC) (°C)	Viscosity (Pa s)[a]	Viscosity ratio ($\eta_{POM} = 505$ Pa s)
PS/PPE 100/0	PS	102	255	1.98
PS/PPE 85/15	Ha4	114	323	1.56
PS/PPE 60/40	Ha6	134	1303	0.39
PS/PPE 50/50	Ha7	144	2068	0.25
PS/PPE 40/60	Ha8	156	3436	0.15

[a] Melt-viscosity at 260°C and shear rate of 50 s^{-1}.

a list of the prepared miscible amorphous phases and their corresponding T_g's.

For all materials, the melt-viscosity under processing conditions was measured using a high pressure capillary rheometer Rheograph 2002 (Göttfert) with a capillary die of 1 mm diameter and *L*/*D* ratio of 30. Measurements were performed at 260°C over a shear rate range, $\dot{\gamma}$, between 10 and 500 s^{-1}. Measurements for a Bagley correction have been performed with capillary dies having an *L*/*D* ratio of 20/1 and 10/1. For the shear rate used to calculate the viscosity ratios ($= 50\ s^{-1}$), the Rabinowitch correction factor was negligible for the lower viscosity materials, i.e. PS E680 and Ha4, and became more important for the more viscous materials; the Bagley correction turned out not to be necessary. The characteristics of all PS/PPE blends are listed in Table 2.

2.3. Compounding of the POM/(PS/PPE) blends

Prior to the melt-blending operations, all materials were dried under vacuum overnight. The materials were then melt-blended in a mini-extruder (DSM Research, The Netherlands), which is a conical co-rotating fully intermeshing twin-screw extruder, with a capacity of about 4 cm^3. A recirculation channel allows the blending time to vary. All blends were prepared under nitrogen atmosphere to prevent oxidative degradation.

Blending conditions were chosen carefully by variation of rotor speed, blending temperature and mixing time. The optimal blending conditions resulting in a well dispersed phase morphology for both low and high viscosity materials, were a mixing temperature of 260°C during 5 min at a screw speed of 50 rpm. After blending, the extruded strand was immediately quenched at the die exit in an isopropanol/solid CO_2 mixture.

POM/(PS/PPE) blends were prepared for POM/PS, POM/Ha4, POM/Ha6, POM/Ha7 and POM/Ha8. Blend compositions (in wt.%) were 60/40, 40/60, 30/70, 20/80, 15/85, 10/90 and 5/95.

2.4. Morphological analysis

To be able to correlate the crystallization behavior of POM in the POM/(PS/PPE) blends with the blend phase morphology, all blends were subjected to the same thermal treatment as used during dynamic crystallization measurements in DSC, prior to phase morphology analysis. Extruded strands were therefore thermally treated in a Mettler hot-stage with FP-90 central processor.

A Scanning Electron Microscope, SEM, (Phillips XL20), operated at an accelerating voltage of 20 kV, was used to examine the particle size and distribution of the dispersed phase. Fracture surfaces perpendicular to the extrusion direction were obtained by brittle fracture in liquid nitrogen. All samples were dried and subsequently coated with a conductive gold layer.

Image analysis of the SEM micrographs was performed with the Leica Quantimet 600 software, giving for each particle the particle area and perimeter, and the longest and smallest distance within the particle. For statistical reasons, at least six SEM micrographs spread well over the sample core region were analyzed, each containing on average 100–200 dispersed domains. By averaging over all micrographs of a blend, reliable data for the mean equivalent particle diameter ($= 2\sqrt{(\text{area}/\pi)}$), the particle size distribution, the number of particles per vol% POM, the total interfacial area and interfacial area per vol% POM and the mean length to breadth ratio could be extracted for further correlations with the crystallization behavior of the blends.

As the SEM micrographs only give information on the sample morphology perpendicular to the extrusion direction, solubility experiments were performed to assess the region of phase inversion. Thermally treated samples were immersed for 2 h in chloroform, which is a solvent for the PS/PPE phase. Only in the case the POM phase forms a co-continuous network structure, the sample will retain its original shape.

2.5. Thermal analysis

Dynamic DSC measurements were performed on a Perkin Elmer Delta series DSC7. Calibration was performed with indium ($T_m = 156$°C) and benzophenone ($T_m = 48$°C). Samples were first heated at a rate of 10°C/min to a melt temperature of 200°C, and kept there for 2 min in order to erase all thermal history. Subsequently, the samples were cooled dynamically at 10°C/min to 50°C whilst recording the dynamic crystallization behavior. Melting experiments

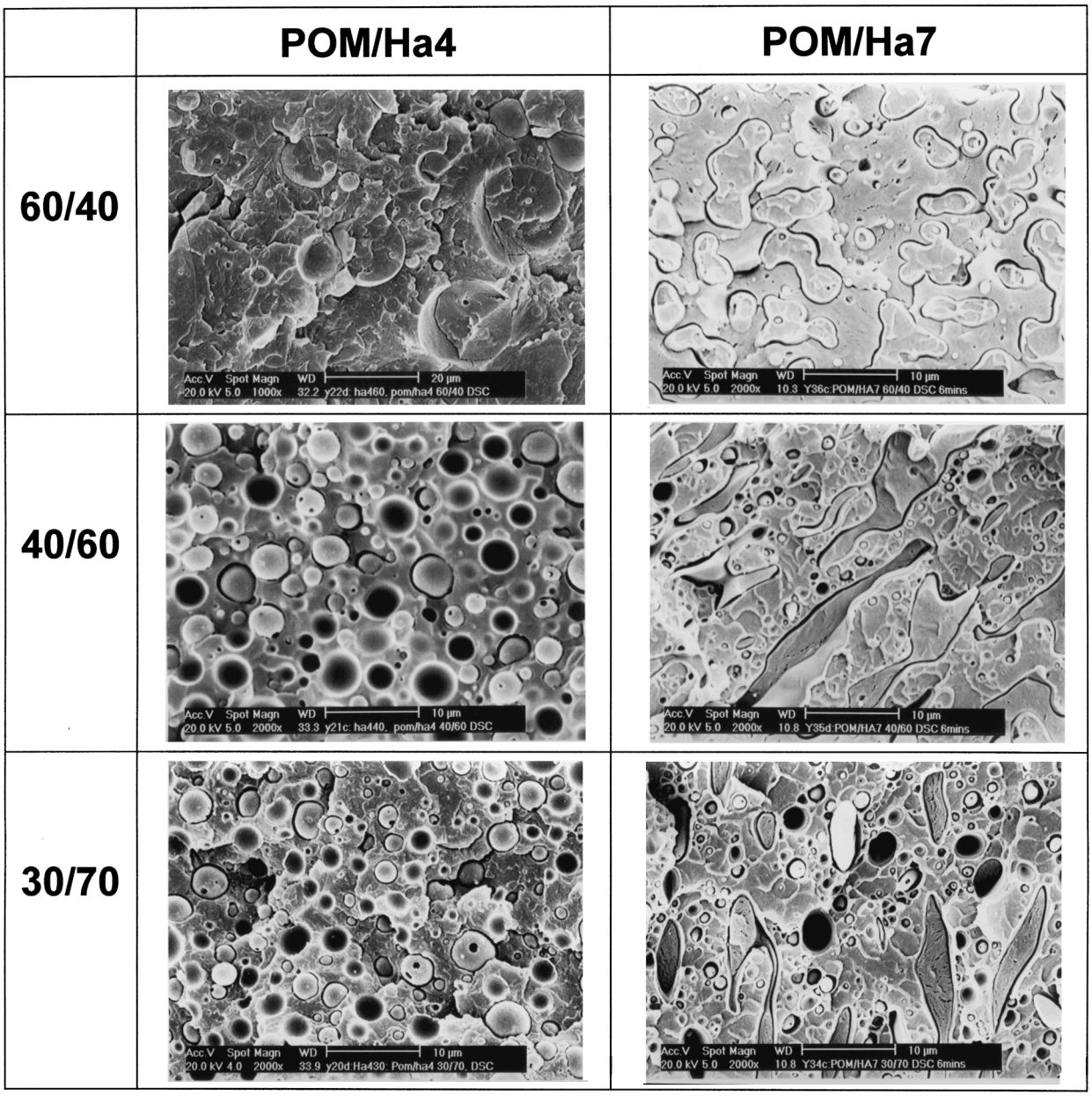

Fig. 2. Blend phase morphology in POM/(PS/PPE) blend systems as a function of blend composition. POM/Ha4 blends are representative for low viscous/low viscous blend systems, POM/Ha7 blends are representative for low viscous/high viscous blend systems.

from 80 to 200°C at a rate of 10°C/min allowed to assess the corresponding melting characteristics of the controlled crystallized blends.

3. Results and discussion

3.1. Phase morphology of thermally treated POM/(PS/PPE) blends

The blend phase morphology of a typical low viscosity/low viscosity (LL) blend series (i.e. POM/Ha4) and a typical low viscosity/high viscosity (LH) blend series (i.e. POM/Ha7) is represented in Fig. 2. The phase morphology of POM/PS or POM/Ha6 and POM/Ha8 blends is not displayed, but behaves quite similar to that observed in POM/Ha4 or POM/Ha7 blends, respectively. A schematic representation of the phase morphology of all blends under investigation is given in Fig. 3.

It is clearly illustrated that a change in the *viscosity ratio* for the same blend composition has a significant effect on the blend phase morphology and on the region of phase inversion. Low viscosity/low viscosity polymer blends (LL blends) always developed a simple droplet-in-matrix morphology of POM droplets dispersed in the miscible amorphous PS/PPE matrix when less than 50 wt.% POM

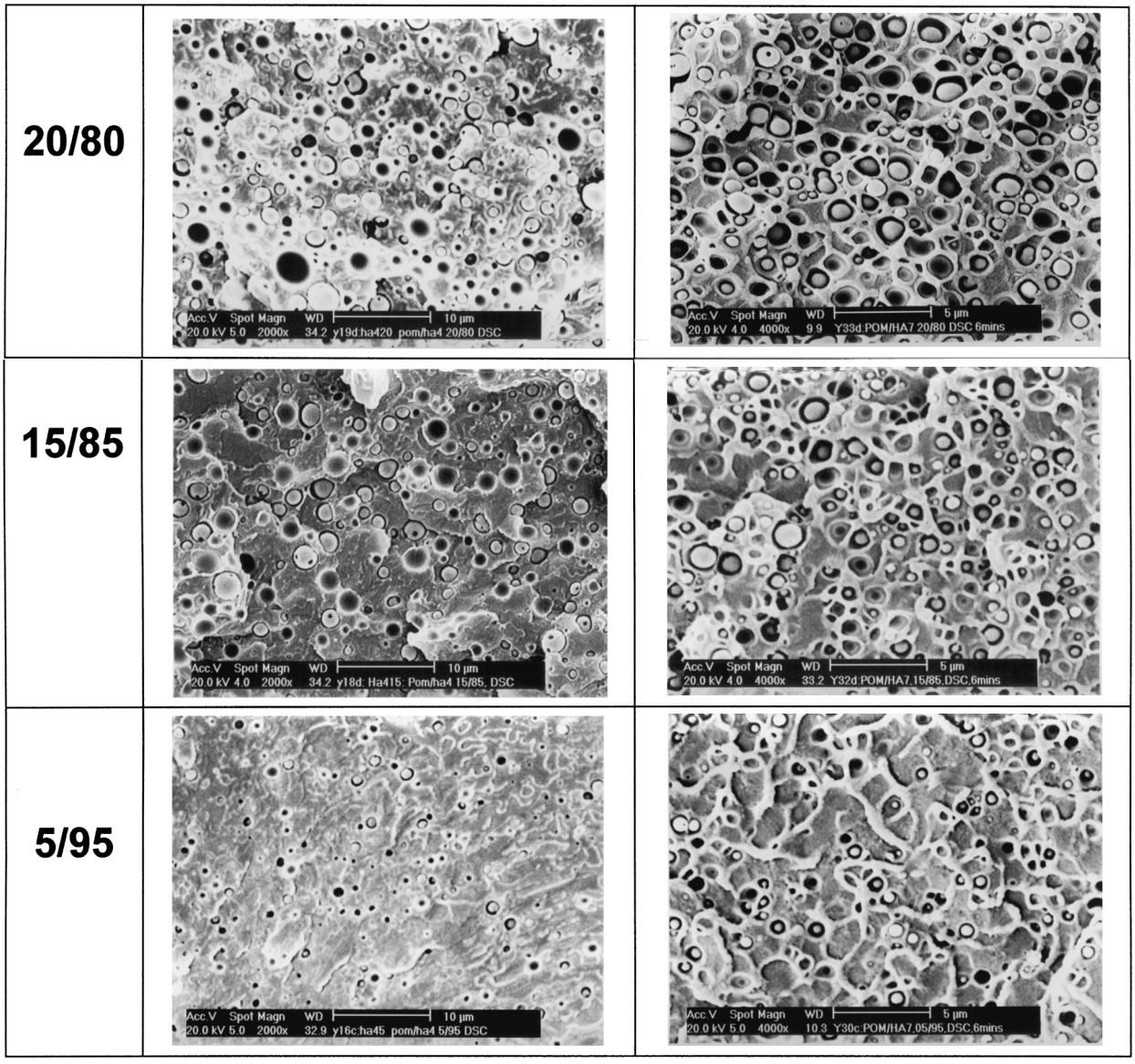

Fig. 2. (*continued*)

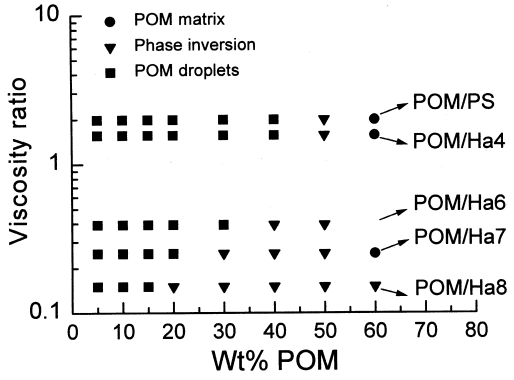

Fig. 3. Schematical overview of the blend phase morphology in POM/(PS/PPE) systems as a function of blend composition and melt-viscosity ratio.

was present. Adding lower amounts of POM consequently resulted in the formation of smaller POM droplets.

Blends of POM with Ha6 (PS/PPE 60/40), Ha7 (PS/PPE 50/50) and Ha8 (PS/PPE 40/60) show an extremely fine dispersion at the lowest concentrations of POM. The lower the melt-viscosity ratio of the blend, the finer the average droplet size of the dispersed POM phase. On account of the preset condition of constant mixing parameters (mixing time, temperature and screw speed), a higher mixing energy input is provided for more viscous materials; high shear stresses are exerted by the highly viscous matrix phase leading to a better droplet break-up and less coalescence.

In the case of low viscosity/high viscosity polymer blends (LH blends) with somewhat higher contents of POM, a broad region of phase inversion exhibiting a complex

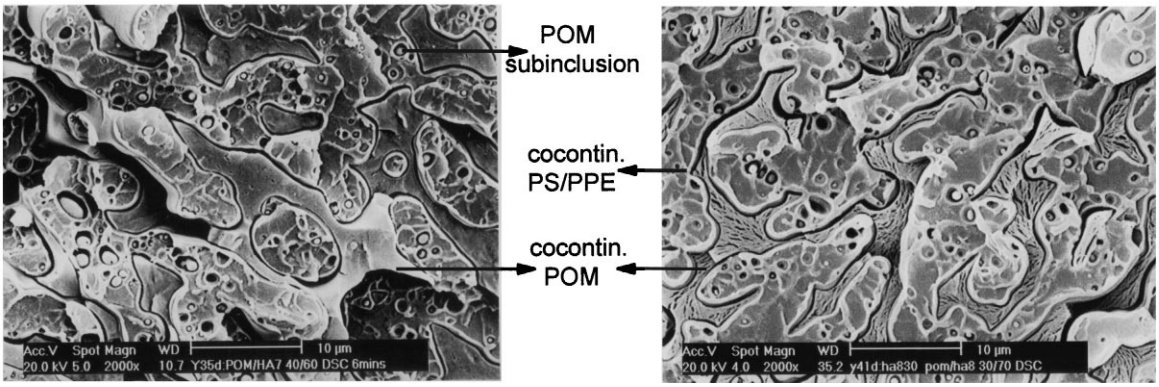

Fig. 4. Complex composite-like phase morphology observed typically in the region of phase inversion of high viscous/low viscous blend systems: (a) POM/Ha7 40/60; (b) POM/Ha8 30/70.

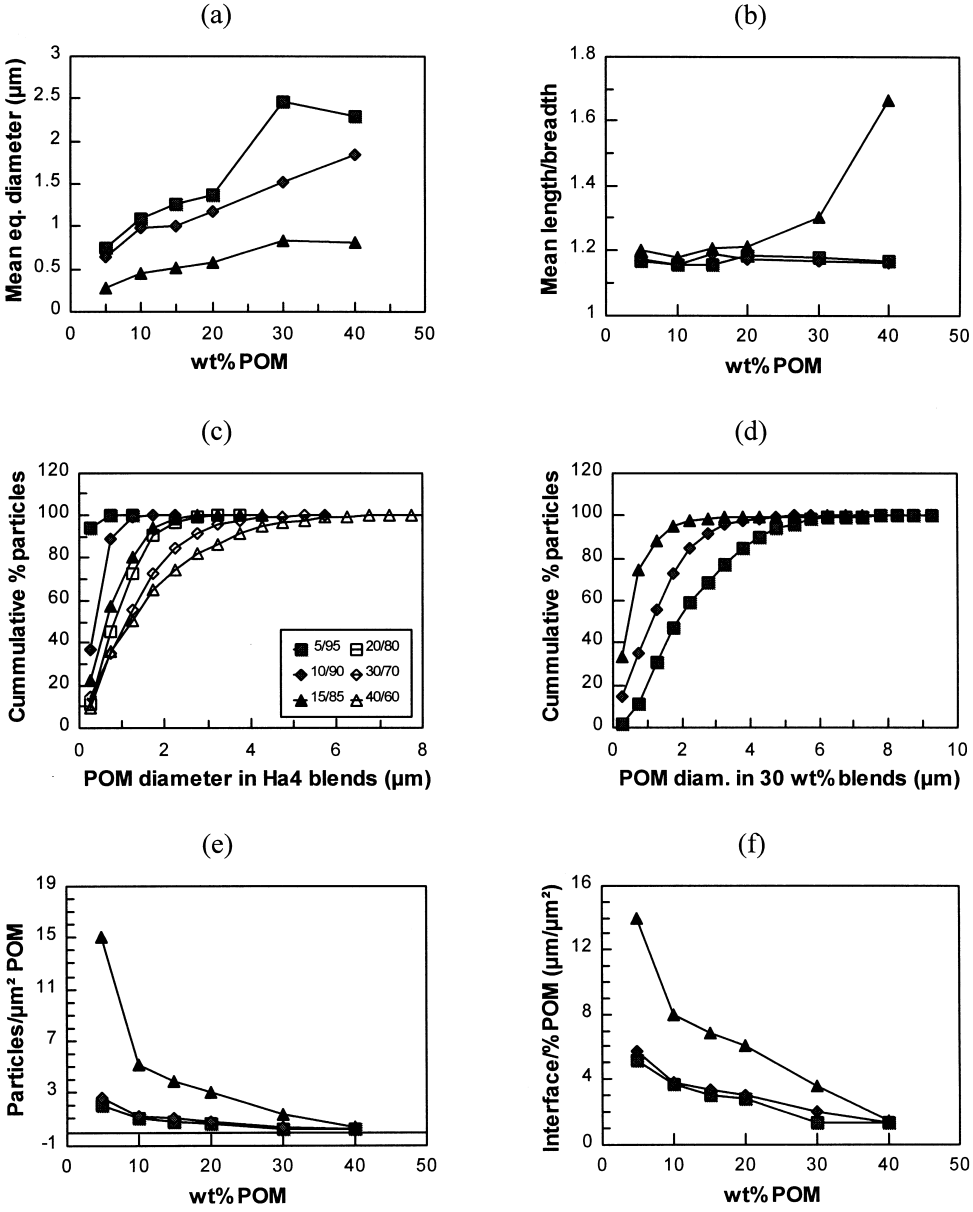

Fig. 5. Overview of the morphological characteristics in immiscible POM/(PS/PPE) blends. (□) POM/PS blends; (◆) POM/Ha4 blends; (▲) POM/Ha7 blends; unless other legends are displayed on the graph.

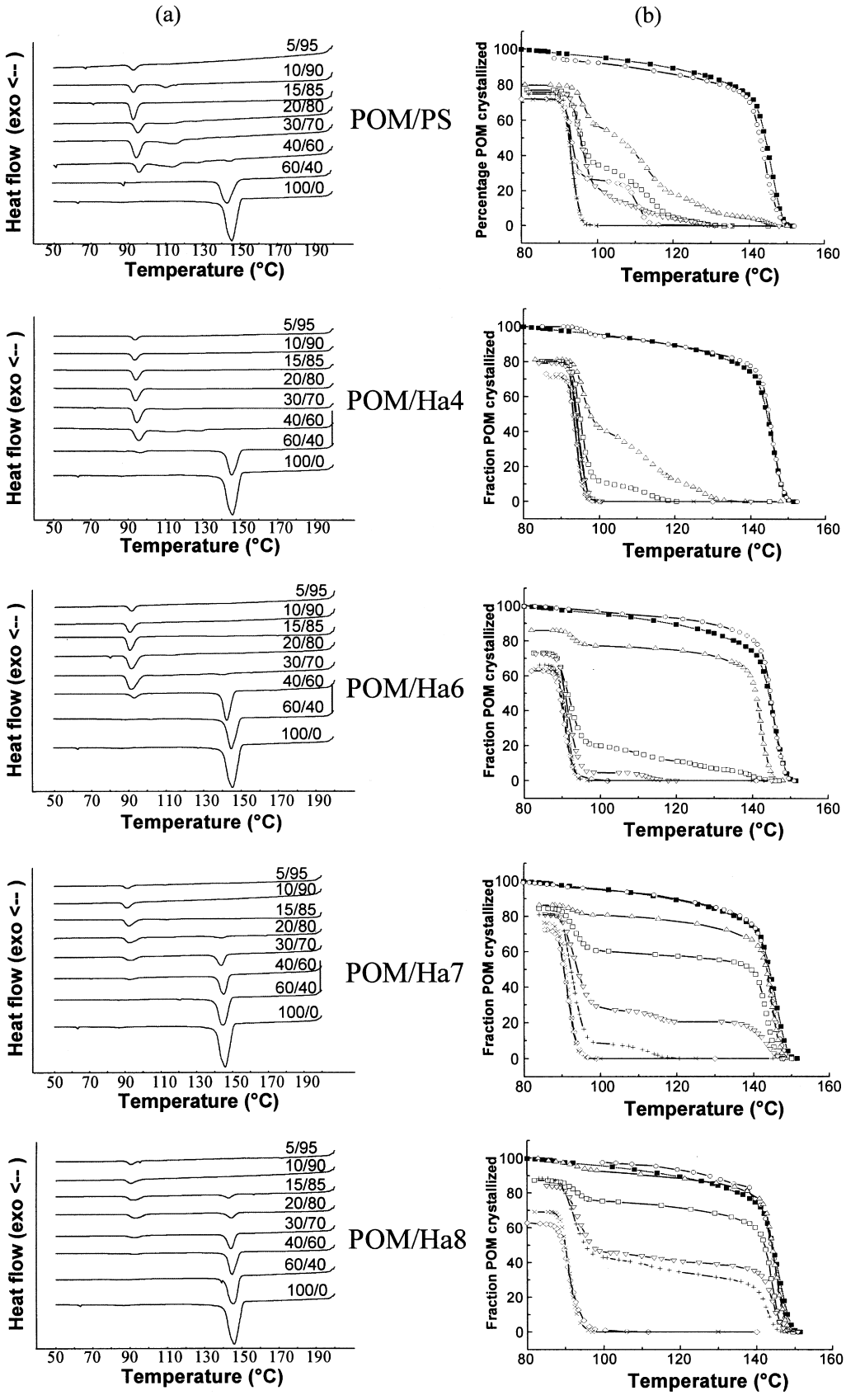

Fig. 6. Dynamic crystallization behavior in POM/(PS/PPE) blend systems. (a) Dynamic DSC traces. (b) Integrated DSC curves normalized to the degree of crystallinity for pure POM (■), and POM/(PS/PPE) 60/40 (○), 40/60 (△), 30/70 (□), 20/80 (▽), 15/85 (+), 10/90 (◇) and 5/95 (×).

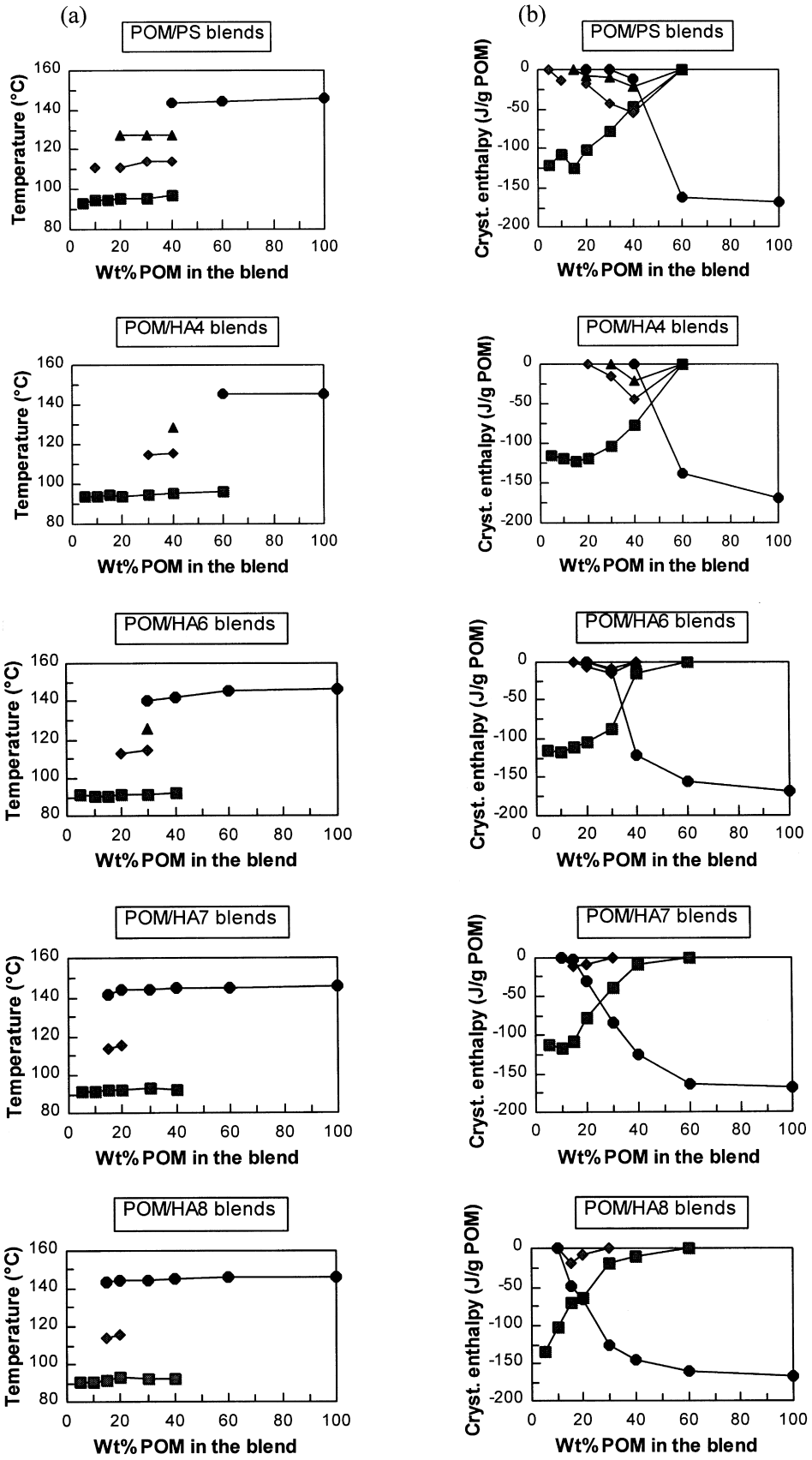

Fig. 7. Overview of the fractionated crystallization behavior in POM/(PS/PPE) blend systems as a function of blend composition: (a) multiple crystallization temperatures; (b) crystallization enthalpy at each discrete crystallization temperature. (●) heterogeneous bulk crystallization around 145°C; (▲) heterogeneous crystallization around 127°C; (◆) heterogeneous crystallization around 114°C; (■) homogeneous crystallization around 91°C.

composite-like phase morphology is observed. Even at a low concentration of 20 wt.% POM, the highly viscous Ha8 phase forms a dispersed-like phase of large, irregular domains which contain a considerable amount of POM subinclusions; the remaining part of the POM phase forms a co-continuous phase (Fig. 4). This peculiar phase morphology can be observed over a broad composition range, i.e. from 20 wt.% POM till even 60 wt.% POM in the POM/Ha8 blends. The formation of a similar composite-like blend morphology has been reported and interpreted extensively for PP/(PS/PPE) blends [1]. It seems that the phase inversion in these blends is most likely retarded by the presence of the highly viscous (slowly softening) PS/PPE 60/40 (Ha6, $T_g = 135°C$), PS/PPE 50/50 (Ha7, $T_g = 144°C$) and PS/PPE 40/60 (Ha8, $T_g = 156°C$) phase. Only partial phase inversion is gradually proceeding until the viscous Ha6, Ha7 or Ha8 phase becomes the matrix. During melt-mixing, the low viscosity POM phase acts as a lubricant to minimize the energy of mixing, and hence retards the liquefaction process of the higher softening phases Ha6, Ha7 and Ha8 [23]. Similar results have been reported by Sundararaj et al. [24,25]. These authors assigned this phenomenon to a difference in softening temperature between both components. The lower melting component will always first encapsulate the higher melting component to form the matrix phase; only if a substantial amount of the higher melting component has softened, gradual phase inversion can proceed, causing this complex composite-like phase morphology. The higher the melt-viscosity and glass-transition temperature of the major component, the longer the time required before a complete equilibrium phase morphology can be attained, and the broader the region of phase inversion observed after a constant mixing time.

The results of a quantitative evaluation of the blend phase morphology of POM/(PS/PPE) blends as a function of blend composition and melt-viscosity ratio are presented in Fig. 5.

As expected, most blends show an increase of the average particle diameter, along with a broadening of the particle diameter distribution, as the amount of dispersed phase increases. This is typically related to droplet coalescence during melt-mixing which is known to be a random process, hence broadening the particle size distribution [26,27]. As a direct consequence, the total number of dispersed POM droplets per volume percentage of the POM phase will increase with decreasing amounts of POM in the blends. Because of the very fine phase morphology obtained in LH blends (i.e. POM/Ha6, POM/Ha7 and POM/Ha8), the number of POM droplets per volume unit POM and the total amount of interfacial contact area per volume unit POM significantly increases with decreasing contents of the POM phase. It can be expected that this will have a pronounced effect on the crystallization behavior of the latter droplets. From Fig. 5(f) the deviation of the mean length to breadth ratio from the value obtained in clearly spherical droplet dispersions, in the 30/70 and 40/60 wt.% POM/Ha7 blends, indicates again that the blend phase morphology here is of the complex composite type where small subinclusions of POM dispersed in co-continuous Ha7 domains co-exist with a co-continuous POM phase.

Because the phase morphology in POM/(PS/PPE) blends behaves similar to the one observed in the previously investigated PP/(PS/PPE) blends [1], no further fundamental understanding of the blend phase morphology development in POM/(PS/PPE) blends will be given here. A more qualitative understanding of all phenomena is given in our paper on this topic [1].

3.2. Fractionated crystallization behavior in POM/(PS/PPE) blends

Dynamic crystallization experiments on POM/(PS/PPE) blends have been performed in a DSC in order to evaluate the influence of blending on the crystallization parameters of the POM phase (T_c, ΔH_c, X_c, etc.). The DSC traces and the corresponding integrated curves are presented in Fig. 6(a) and (b), respectively.

It can be clearly seen that the crystallization of POM is drastically affected by melt-blending, especially at lower contents of POM. Fractionated crystallization can be observed for all blend types, with a clear compositional dependence. It is however clear that the blend composition as such does not play the determining role, as a comparison of the same blend composition in the different blend types under investigation, yields very different crystallization curves. LL blends (i.e. POM/PS and POM/Ha4) for example display multiple crystallization peaks over a broad composition range, whereas LH blends (i.e. POM/Ha7 and POM/Ha8) generally only crystallize at two discrete steps, being the bulk crystallization temperature for POM around 145°C and the homogeneous crystallization temperature for POM around 92°C [4]. Further, a gradual decrease of the intensity of the bulk crystallization peak along with the increase of other crystallization exotherms is observed when the content of POM decreases. A schematic representation of the impact of fractionated crystallization in blends with decreasing content of the crystallizable POM phase is given in Fig. 7.

First of all, it is obvious that melt-blending small amounts of a crystallizable component with other immiscible materials has a drastic impact on its *crystallization temperature*.

Crystallization peaks of the dispersed POM droplets are observed only at four discrete temperatures (Fig. 7(a)). These peaks can be assigned as a normal bulk crystallization peak around 145°C, where the nucleation has started from heterogeneities with the lowest specific interfacial energy difference, Δy_1 (regime II nucleation). Such heterogeneities are typically catalyst residues, impurities, etc. Frensch et al. [7] stated that multiple crystallization peaks reflect the efficiency spectrum of the several nucleating heterogeneous species available in the crystallizable phase. Heterogeneities with the lowest activation energy, ΔF_1^*, and the lowest

specific undercooling, $\Delta T_{c,1}$, under normal conditions become active at the bulk crystallization temperature of POM (145°C). Once sufficiently primary nuclei of critical size are available, crystallization can spread out over the whole bulk material via secondary nucleation (crystal growth). However, in polymer blends containing only discrete droplets of the crystallizable phase, secondary nucleation is restricted to the confined volume of the droplet. Other droplets, which do not contain sufficient heterogeneities of this type are nucleated at much higher degrees of undercooling. It is believed that droplets become depleted in heterogeneities of the first type as soon as the total number of dispersed droplets exceeds the number of heterogeneities with the lowest activation energy [7,10]. As such, droplets which do not contain nuclei of the type 1 will not crystallize at $T_{c,bulk}$, and upon further cooling from the melt, heterogeneities requiring a higher activation energy have the opportunity to become active and act as nucleating substrate.

The homogeneous crystallization temperature, $T_{c,hom}$, of a material can be estimated roughly from the generally applicable Eq. (1), an empirical relationship established for metals [28].

$$T_{c,hom} = 0.8T_E, \quad (1)$$

with T_E the melt/crystal equilibrium temperature (in K). In the case of polymeric materials, T_E can be taken as the veritable melting temperature, T_m [48]. According to Eq. (1), $T_{c,hom}$ for POM should hence be found around 90°C. The lowest observable crystallization peak in our DSC curves is found around 94°C in LL blends and around 91°C in LH blends. These temperatures agree fairly well with the experimentally observed crystallization temperature in finely dispersed POM droplets by Koutsky et al. [4]. It hence can be readily accepted that homogeneous nucleation has occurred around 91°C. Further, from Fig. 6(b), it can be observed that the conversion rate at this temperature is much faster than the one observed for the intermediate crystallization temperatures or even for bulk crystallization. This confirms again the fundamental difference in the nucleation and/or growth mechanism when POM is crystallizing around 91°C and only can be understood if homogeneous nucleation is assumed. Hoffman and Weeks [29] reported a similar catastrophic nucleation behavior resulting in the formation of extremely small folded chain crystals when polychlorotrifluoroethylene was crystallized at a supercooling of 70°C or higher, and assigned this to be due to homogeneous nucleation. Similar observations were reported for polyethylene droplets crystallizing around 85°C [30]. The authors experimentally demonstrated that the spherulite growth rate in homogeneous crystallizing PE droplets is so high that only a regime III nucleation mode is possible, where the rate of nucleation is so high that there is a lack of space for lateral growth. If, further, the chain mobility becomes somewhat restricted due to the high degrees of undercooling, only small and imperfect crystal structures can develop. Vonnegut [19] stated that in the case of small droplets, the crystallization rate at the homogeneous crystallization temperature usually is so large that a single nucleus could crystallize the whole droplet.

Two other crystallization peaks sometimes can be observed around 127 and 114°C. Similar observations were reported by Klemmer and Jungnickel [5] for extruded immiscible blends where POM was dispersed in a HDPE matrix. A bulk crystallization peak was detected at 144°C, and an additional peak of delayed crystallizing POM droplets was found at 130°C. The latter had been attributed by the authors to an interface-induced additional inhomogeneous nucleation. The position of these subsidiary peaks slightly shifted to lower temperatures with lower contents of POM. A similar observation could be seen in the POM/(PS/PPE) blends under investigation (Fig. 7(a)). These peaks must be the result of heterogeneously nucleated droplets, where the specific interfacial energy difference, Δy_i, of the active heterogeneities is somewhat higher than for those active at $T_{c,bulk}$, and thus require a higher degree of undercooling. It is believed that this type of heterogeneities are typically smaller and/or less perfect heterogeneous nuclei which can grow in time to a critical size, but still remain limited in number [31].

In Fig. 7(b), the evolution of the *crystallization enthalpy* at each fractionated crystallization step is displayed as a function of the weight percentage POM. It has to be noticed that the bulk crystallization and homogeneous crystallization peaks are responsible for the major fraction of crystallized material. The intermediate crystallization peaks around 127 and 114°C only account for a minor fraction of the crystallized POM, and are less important in the LH blend series. A smooth and gradual decrease of the bulk crystallization enthalpy along with an increase in intensity of the homogeneous crystallization enthalpy is observed with decreasing POM contents in the blends. The enthalpy of the intermediate heterogeneously nucleated POM peaks displays a maximum around the cross-over point of bulk and homogeneous enthalpy functions. This observation agrees

Table 3
Influence of the POM content in POM/(PS/PPE) blend systems on the final degree of crystallinity, X_c, as calculated directly from fractionated crystallization curves. X_c for POM is 54%

Wt.% POM	POM/PS	POM/Ha4	POM/Ha6	POM/Ha7	POM/Ha8
5	42[a]	41[a]	40[a]	39[a]	47[a]
10	42	41[a]	41[a]	41[a]	36[a]
15	43[a]	43[a]	39[a]	43	46
20	43	41[a]	39	41	46
30	44	41	42	41	47
40	45	48	45	44	51
60	53[b]	46	51[b]	53[b]	52[b]

[a] Only one crystallization exotherm around 95°C (homogeneous nucleation).

[b] Only one crystallization exotherm around 145°C (bulk nucleation).

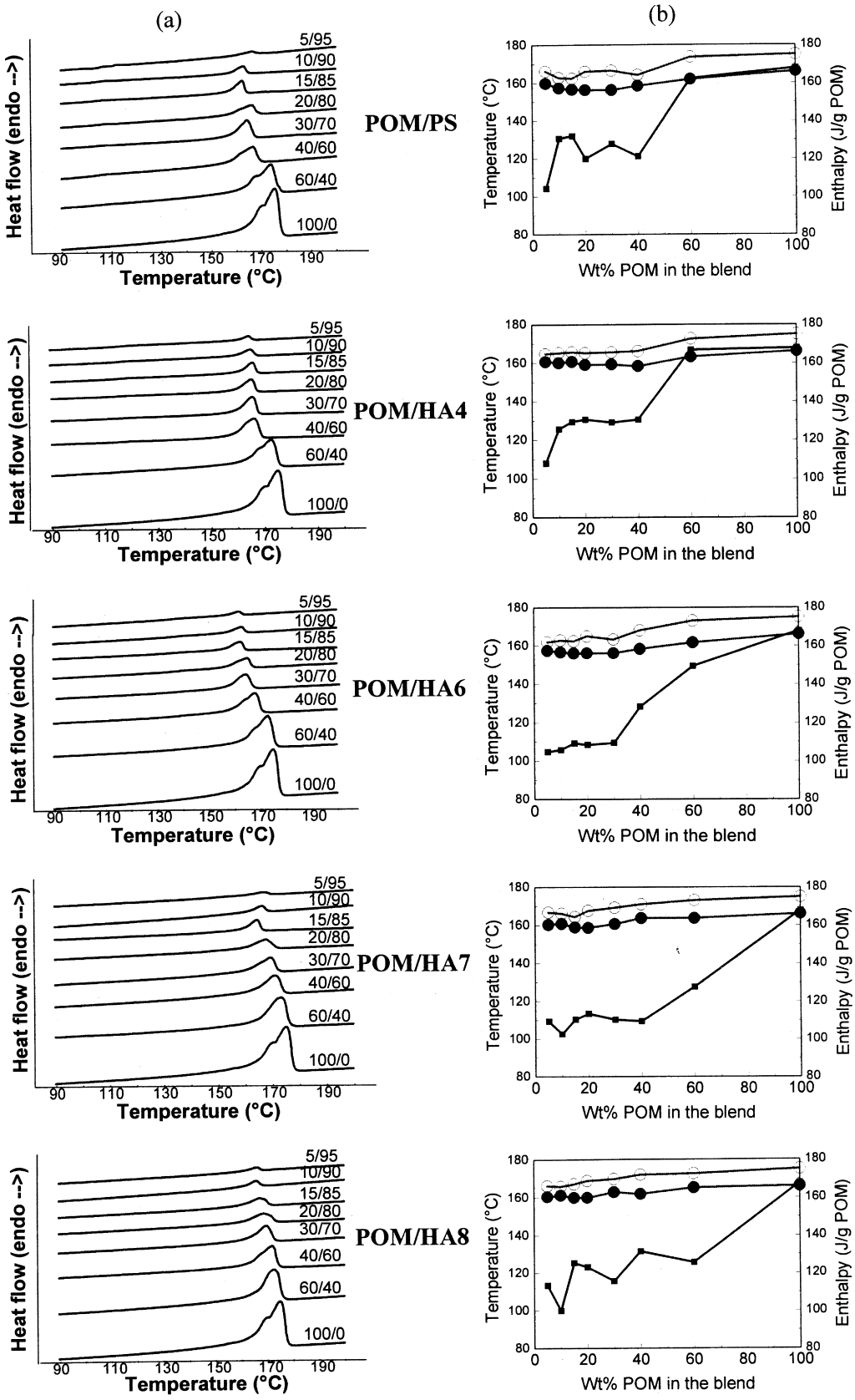

Fig. 8. Melting behavior of fractionated crystallized POM/(PS/PPE) blend systems: (a) dynamic DSC traces; (b) melting temperature and enthalpy. (○) temperature of the maximum in the melting peak; (□) onset temperature of melting; (■) melting enthalpy (J/g POM).

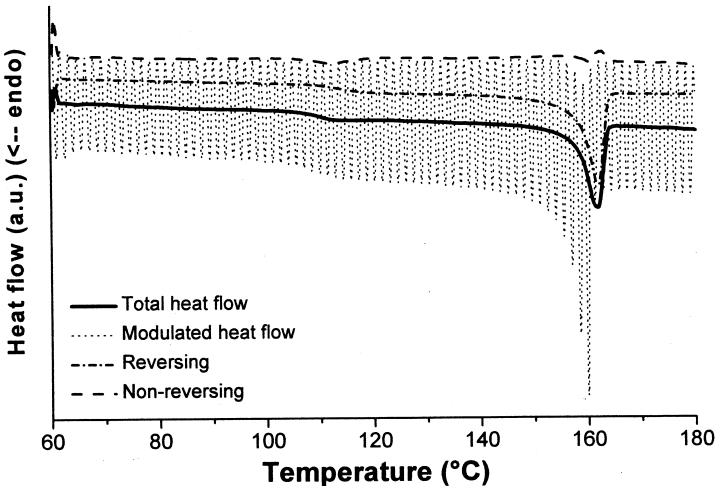

Fig. 9. Modulated DSC traces of a POM/Ha4 20/80 blend. No recrystallization can be observed in the non-reversing signal upon melting.

well with the results found by Klemmer and Jungnickel [5] in HDPE/POM blends.

The crystallization enthalpy, ΔH_c, observed for fully homogeneously crystallizing POM droplets (± -115 J/g POM) never seems to attain the same value as ΔH_c for fully bulk crystallized POM (± -165 J/g POM). This implies a reduction of the degree of crystallinity, X_c, with on average 30%. Even when taking into account a correction factor for the temperature dependence of the reference enthalpy function [32–34] (Eq. (2)), where ΔH_c^0 at $T_{c,hom}$ is more than 25 J/g POM lower than the commonly accepted reference enthalpy of 315 J/g POM at $T_{c,bulk}$, a global decrease in X_c of about 25% still can be observed in blends at low contents of POM (Table 3).

$$\Delta H^0(T) = -0.0013T^2 + 1.4587T - 70.838, \quad (2)$$

where T is the temperature in Kelvin.

As long as the crystallizable phase remains the matrix, as is the case for all blend series at a 60/40 POM/(PS/PPE) composition, the degree of crystallinity remains unaffected around 54%, as there is only crystallization at the bulk T_c. From the point multiple crystallization peaks are observed, X_c starts to level off, to finally attain a value of about 40% in fully homogeneously crystallizing samples, independent of the dispersed particle size.

This behavior is confirmed from the corresponding *melting behavior* of the POM/(PS/PPE) blends. Fig. 8 shows the melting traces of fractionated crystallized blends as recorded by DSC, and the evolution of the melting peak temperature and melting enthalpy as a function of the weight percentage POM in the blends. The evolution of the total melting enthalpy as a function of the wt.% POM corresponds fairly well with the tendency observed during crystallization; lower contents of POM in the blends lead to more homogeneous crystallization and a lower degree of crystallinity. The depression of the melting enthalpy, ΔH_m, in POM/(PS/PPE) blends with intermediate contents of POM seems to be more pronounced in POM/Ha6 and POM/Ha7 blends than in POM/Ha8 blends; ΔH_m is least depressed in POM/PS and POM/Ha4 blends.

It can be observed that decreasing amounts of POM not only lead to a lower melting enthalpy, but also cause the onset of melting to be shifted towards lower temperatures (on average 10°C) with respect to the melting peak of the POM homopolymer. From modulated DSC experiments, it could be seen that recrystallization phenomena are not observed, and thus can not alter the original lamellar texture of the fractionated crystallized samples during the heating run (Fig. 9). This agrees with the findings of Blais and Manley [35], who observed no recrystallization of POM below 171°C when gradually heating. Fast heating of the same POM to temperatures above 171°C however did cause extensive recrystallization phenomena.

A clear reflection of the crystallization behavior could be seen from the melting endotherms. Purely homogeneously nucleated samples, as is the case for all POM/(PS/PPE) blends with a 5/95 and 10/90 composition, only showed one single melting endotherm around 165°C. In samples that underwent both homogeneous and heterogeneous crystallization at higher degrees of undercooling, a shoulder at the high temperature side of the homogeneously nucleated melting endotherm appears and gradually increases with decreasing importance of the homogeneous crystallization peak. Once heterogeneous crystallization at $T_{c,bulk}$ starts to play a role, often a double melting peak with a small shoulder at its lower temperature side appears. Both peak positions are strongly shifting to higher temperatures with increasing amount of POM crystallizing at $T_{c,bulk,}$ until the peak position of the shoulder reaches 170°C and the main melting peak attains 175°C. The lower temperature shoulder in the melting endotherm of bulk crystallized samples becomes more pronounced when a broad low temperature crystallization exotherm around 88°C was observed during cooling from the melt (i.e. in POM pure, POM/PS 60/40 and POM/Ha4 60/40 blends). The latter has been attributed in

the literature to the 'defect' chain segments in copolymers—the POM used in this study has been stabilized against degradation by copolymerization with 5 wt.% ethyleneoxide- which do not fit the crystal structure formed during primary crystallization. Such perturbed sequences only can crystallize at degrees of undercooling that are high enough so that the side chain length of the copolymer becomes larger than the critical crystallite thickness for crystallization at that temperature [36].

As melting curves in which no recrystallization takes place during heating are the reflection of the melting of the originally formed crystalline lamellae, the shift of the melting peak towards lower temperatures is most probably related to the formation of smaller and less perfect crystalline lamellae during the faster crystallization at much higher degrees of undercooling. A detailed investigation of the lamellar morphology of fractionated crystallized POM/(PS/PPE) blends where the POM phase is the minor component has been performed and will be discussed in the next part of this paper [37].

3.3. Morphological and physical parameters influencing the crystallization behavior of POM/(PS/PPE) blends

In the present study, a series of immiscible blends of POM with miscible PS/PPE compounds are investigated. By simply varying the PS/PPE composition, changes in both the blend phase morphology (by the altered viscosity ratio) and the physical state of the amorphous matrix phase (due to a change in T_g) can be introduced at constant blend compositions in a controlled way, without affecting the interfacial tension of the blend system [22]. The latter allows to evaluate the parameters affecting the degree of fractionated crystallization in immiscible POM/(PS/PPE) blends.

It is clear from Fig. 6 that the fractionated crystallization behavior can be very different depending on the blend series under investigation. At first glance, the *content* of the crystallizable POM phase in the blends plays a crucial role with respect to the extent of fractionated crystallization. Decreasing the POM content always causes a more intense homogeneous crystallization. However, there does not seem to be any direct relationship between the amount of the crystallizable phase and the crystallization behavior recorded by DSC, when comparing different blend series. The reason for this is obvious; fractionated crystallization has been shown to be related to a fine blend phase morphology, in which the total number of dispersed crystallizable droplets exceeds the number of heterogeneities with the lowest activation energy, normally active at $T_{c,bulk.}$ This explanation is often accepted as the sole reason behind fractionated crystallizing polymer blends [7]. As each blend series has a different melt viscosity ratio, different blend phase morphologies are produced at the same blend composition. Morales et al. [13] investigated the relationship between blend phase morphology and crystallization behavior in immiscible polymer blends. These authors stated that simple DSC measurements look very promising as a straightforward tool to estimate the state of dispersion in immiscible polymer blends where the minor phase exhibits fractionated crystallization. However, it becomes directly clear from Fig. 6 and from the blend phase morphology discussed previously, that this is a much too simplistic approach of the phenomenon of fractionated crystallization. For all the blend series, a clear droplet-in-matrix morphology is observed at low concentrations of POM, with the size of the dispersed POM phase being much smaller in POM/Ha8 blends compared to POM/Ha4 blends. Comparison of the DSC traces of both blend series however reveals surprisingly that the POM/Ha8 blends are the least sensitive to fractionated crystallization, as bulk nucleation can be observed up to a POM/(PS/PPE) 15/85 blend composition, whereas in the case of POM/Ha4 blends no more bulk nucleation is appreciable from a 40/60 POM/(PS/PPE) composition onwards. The latter observation leads us to the conclusion that other factors, besides the blend phase morphology and nucleation density of the crystallizable phase, must play a role in the way the dispersed phase is crystallizing upon cooling from the melt. A careful and quantitative evaluation of all crystallization parameters thus is required to understand the influence of blending on the fractionated crystallization behavior in POM/(PS/PPE) blends with different amorphous PS/PPE matrix phases.

For a complete and thorough understanding of the driving forces behind fractionated crystallization, several questions now arise and need to be answered: (i) What determines the onset of fractionated crystallization and/or the offset of heterogeneous nucleation at $T_{c,bulk}$? (ii) Is fractionated crystallization solely related to the blend phase morphology? (iii) Under what conditions are multiple crystallization peaks (i.e. the subsidiary exotherms observed around 127 and 114°C) possible, and what determines the number and extent of multiple crystallization peaks? (iv) What causes the decrease of the crystallinity in fractionated crystallizing samples?

3.3.1. What determines the onset of fractionated crystallization and/or the offset of the heterogeneous bulk nucleation peak?

The onset of fractionated crystallization can be defined as the blend composition at which other crystallization peaks besides the heterogenous bulk crystallization peak appear in the DSC trace. Table 4 gives an overview of all relevant morphological parameters at the onset of fractionated crystallization in the five blend series under investigation.

It is evident from Table 4 that the onset of fractionated crystallization is situated around 40 wt.% POM, independent of the blend series under consideration. As both the size of the dispersion and the number of particles per volume percentage POM differ for each blend series, the latter morphological parameters do not seem to be directly correlated with the onset of fractionated crystallization. It is

Table 4
Morphological characteristics at the onset of fractionated crystallization in POM/(PS/PPE) blends

	POM/PS	POM/Ha4	POM/Ha6	POM/Ha7	POM/Ha8
Onset (wt.% POM)	40 or 50	40 or 50	40	40	40
POM phase	Droplets or cocontinuous	Droplets or cocontinuous	cocontinuous +subinclusions	Cocontinuous +subinclusions	Cocontinuous +subinclusions
Diameter of droplets (μm)	>2.28	>1.84	–	0.82	–
Particles/area% POM (μm^{-2})	<0.18	<0.25	–	0.34	–
Region of phase inversion	50	50	40–50	30–50	20–60
%non-bulk crystallinity	100	100	11	7	6.5

however striking that for all blend series, the onset of fractionated crystallization coincides with the center of the phase inversion region. At this point, the phase morphology is expected to change from a predominantly POM matrix phase to a predominantly dispersed POM phase. This is the point where the majority of the POM phase is split up into separate volumes that are not in contact with each other. Consequently, crystallization can not spread out anymore over the whole POM volume via secondary nucleation, once primary nucleation from a heterogeneity active around $T_{c,bulk}$ has occurred. Phase inversion thus implies a physical barrier against further crystal growth.

A review of the literature published on fractionated crystallizing immiscible polymer blends reveals indeed similar observations in several investigated blend systems. Santana and Müller [10] studied blends of isotactic polypropylene (PP) with polystyrene (PS) over the whole composition range; a first hint of homogeneous crystallization could be observed in the DSC curves at a PP/PS 50/50 composition (although the authors neglected this small peak and only discussed homogeneous crystallization from a 30/70 blend composition onwards). Because both the PS and PP possess rather comparable melt-viscosities, phase inversion is expected indeed around a PP/PS 50/50 composition. Morales et al. [13] investigated PS/LLDPE blends, and found fractionated crystallization to start from a 60/40 blend composition onwards; again, this composition was situated just beyond the region of phase inversion.

A striking difference in behavior between POM/PS or POM/Ha4 on the one side, and POM/Ha6, POM/Ha7 or POM/Ha8 on the other side is registered. In LL blends (i.e. POM/PS and POM/Ha4) the onset of fractionated crystallization implies at the same time a complete disappearance of the bulk crystallization peak, while in the case of LH polymer blends (i.e. POM/Ha6, POM/Ha7 and POM/Ha8) only a small portion of the POM phase is involved in fractionated crystallization. This phenomenon can only be understood in the context of the different mechanism of phase inversion between both blend types. LL blends have been demonstrated previously to be able to provoke a fast and easy phase inversion from a POM matrix with PS/PPE droplets, over a perfectly co-continuous phase morphology, to a PS/PPE matrix with POM droplets [1]. Often, the intermediate co-continuous phase structure is not very stable and grows towards a more stable droplet-in-matrix structure [38]. As a consequence, the crystallizable POM phase will be either present as matrix phase ($\Delta H_{c,bulk} = 100\%$), or as fully dispersed phase ($\Delta H_{c,bulk} = 0\%$). In the case of LH polymer blends, the region of phase inversion corresponds to a complex composite phase morphology where co-continuous POM structures coexist with very fine subinclusions of POM, as a consequence of the slowly developing and difficult (non-equilibrium) phase inversion process [1,24,25]. Hence, only the fraction of POM subinclusions will be involved in fractionated crystallization. It can thus be estimated from DSC measurements that the total amount of POM subinclusions at a POM/(PS/PPE) 40/60 blend composition is more important for POM/Ha6 than for POM/Ha8 blends. Again, this is in agreement with our understanding of the development of the phase morphology in the region of phase inversion; the higher the viscosity ratio of the blend, the higher the amount of PS/PPE required to provoke phase inversion and the lower the volume fraction of POM subinclusions formed at higher contents of POM (i.e. a 40/60 POM/(PS/PPE) composition).

A thorough understanding of the parameters determining the blend composition for the offset of heterogeneous nucleation around $T_{c,bulk}$ is less evident. An overview of the most important parameters is given in Table 5.

From Fig. 6, it could already be seen that LL polymer blends do not display bulk nucleation anymore from the start of the fractionated crystallization. The same explanation as given for the onset of fractionated crystallization in these blends is valid here; fast phase inversion with the formation of a clear droplet-in-matrix morphology causes either a fully bulk nucleated POM matrix, or a fully dispersed POM phase morphology where the intensity of fractionated crystallization is directly determined by the number of POM droplets.

In the case of LH polymer blends (POM/Ha6, POM/Ha7 and POM/Ha8) a clear shift of the offset temperature for bulk nucleation to lower contents of POM can be observed. In the case of POM/Ha8 blends for example, bulk nucleation could be observed up to a 15/85 POM/Ha8 composition. The major reason for this shift in the blend composition at which the last portion of bulk nucleated POM can be observed again must be attributed to the complex composite type of phase morphology in the region of phase inversion. As long as co-continuous POM domains can coexist with POM subinclusions, the former will be able to crystallize

Table 5
Morphological characteristics at the offset of fractionated crystallization in POM/(PS/PPE) blends

	POM/PS	POM/Ha4	POM/Ha6	POM/Ha7	POM/Ha8
Last $T_{c,bulk}$ (wt.% POM)	50 or 60	50 or 60	30	20	15
POM phase	Cocontinuous or matrix	Cocontinuous or matrix	Droplets	Droplets	Droplets[a]
Diameter of droplets (μm)	–	–	–	0.58	–
Particles/area% POM (μm^{-2})	0	0	–	3.02	–
Region of phase inversion	50	50	40–50	30–50	20–60
% crystallinity of bulk peak	100	100	8.2	23.6	33.9

[a] Solubility tests revealed besides the droplet-in-matrix core region, a cocontinuous skin region.

around $T_{c,bulk}$. Further, due to the smaller size of the POM subinclusions in POM/Ha8 blends, as compared to POM/Ha6 blends, the volume fraction of POM involved in fractionated crystallization becomes less important. Consequently, the amount of POM crystallizing by heterogeneous nucleation around $T_{c,bulk}$ in POM/Ha8 blends is found to be larger than in POM/Ha6 blends.

However, the complex composite type morphology in the region of phase inversion of LH polymer blends only seems to explain partly the observed bulk nucleated POM fraction. From Table 5 it is clear that the offset blend composition for heterogeneously nucleated POM is even beyond the region of phase inversion, where all POM should be finely dispersed in discrete droplets (see Figs. 2 and 3). Moreover, blends having a finer dispersed POM phase (i.e. POM/Ha8) show less fractionated crystallization and a higher volume of POM involved in heterogeneous nucleation around $T_{c,bulk.}$ This is just opposite to what would be expected on the basis of the general theory of fractionated crystallization [4,7,8]. Evidently, the question arises whether the limits of the region of phase inversion at low POM contents have been determined fully correctly. From SEM micrographs on brittle fractured samples (Fig. 2), a clear droplet-in- matrix type morphology can be observed. Solubility experiments then were performed with chloroform in order to dissolve all PS/PPE in the blends. The samples in which the last bulk nucleated crystallization peak was observed indeed all fell apart due to a lack of co-continuous network structures, although some parts of the skin seemed to stay together and formed a swollen jelly-like structure. The latter however does not seem sufficient to us to explain the increasing portion of bulk nucleated POM with decreasing melt-viscosity ratio of the blends, or increasing glass transition temperature of the matrix phase. The question thus arises whether additional bulk nucleation at the interface of the solidified PS/PPE matrix could have occurred.

3.3.2. Estimation of the blend phase morphology from the onset of $T_{c,bulk}$

From the previous discussion, it becomes clear that an evaluation of the onset temperature for heterogeneous bulk nucleation in immiscible POM/(PS/PPE) blends can be a valuable tool to estimate the blend phase morphology. From Fig. 6(b), it could already be seen that the temperature at which the steady state for nucleation is reached shifts to higher degrees of undercooling with decreasing content of the crystallizable phase. This retardation of the nucleation process indicates that the total amount of active primary nuclei at $T_{c,bulk}$ gradually decreases with decreasing POM content. Fig. 10 displays the evolution of the onset temperature of the bulk crystallization peak as a function of the weight percentage POM in the blends. The latter gives a better insight into the impact of blending on the nucleation density of the crystallizable phase.

The correlation between the type of blend phase morphology, i.e. a (co-)continuous POM phase or POM droplets, and the onset temperature for bulk nucleation is striking. As long as POM forms the matrix phase, i.e. in POM/Ha 60/40 blends, $T_{c,bulk}$ is not significantly lowered. The slightly lower onset of crystallization (about $-1°C$) can be attributed to the migration of heterogeneous nuclei, active at $T_{c,bulk}$, from the POM phase towards the PS/PPE phase during the melt-mixing process [39–41]. As soon as the POM phase becomes the dispersed or co-continuous phase, $T_{c,bulk}$ is affected more clearly. In LL blends, where the POM phase is always dispersed from a POM/(PS/PPE) 40/60 composition onwards, no more bulk crystallization can be observed. In the LH blends however, $T_{c,bulk}$ is shifted 2–6°C lower than in pure POM, depending on the T_g or melt-viscosity of the sample matrix. This reduction of $T_{c,bulk}$ can be ascribed to the lower amount of material involved in the bulk crystallization process, according to revised overall crystallization kinetics for crystallization in confined volumes [42–45]. Due to the effect of volume limitations, the overall crystallization rate in smaller volumes is reduced compared to the theoretical predictions from the Evans–Avrami theory [46] for an infinite volume. When a constant cooling rate is imposed, a slowing down in the kinetics thus will lead to a decrease in the observed crystallization temperature. The smallest dimensions of a phase will be the rate determining factor for the crystallization kinetics [42]. The blend phase morphology (i.e. matrix, co-continuous or large droplets, and the relative amount of the crystallizable phase involved in bulk crystallization) can thus be roughly estimated from the decrease of the onset temperature for heterogeneous bulk nucleation (Fig. 10).

The decrease of $T_{c,bulk}$ is most pronounced for POM/Ha6 blends, and becomes less important with increasing T_g or

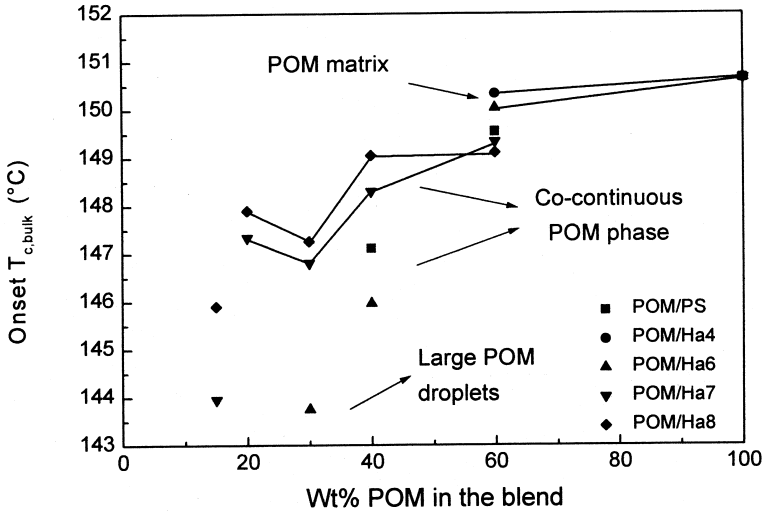

Fig. 10. Estimation of the mode of dispersion and content of POM in POM/(PS/PPE) blend systems from the onset temperature for heterogeneous bulk nucleation.

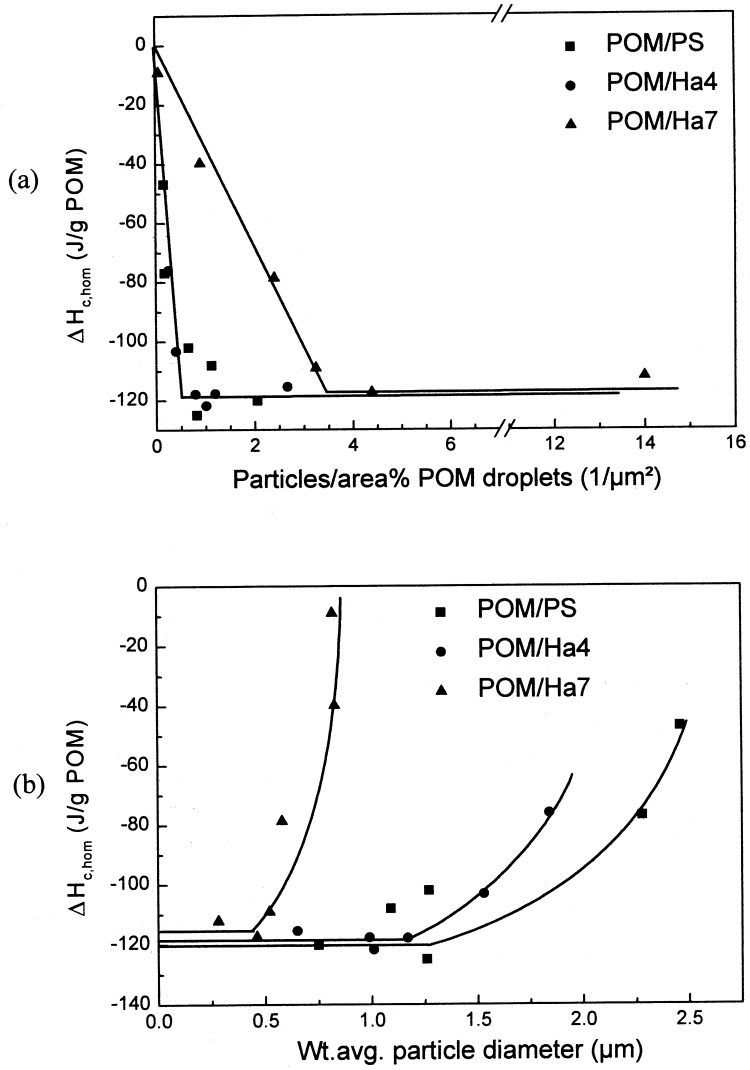

Fig. 11. Influence of: (a) the total number of dipersed droplets per area% POM: and (b) the weight average diameter of POM droplets, on the intensity of fractionated crystallization in POM/(PS/PPE) blend systems.

Table 6
Estimation of the nucleation density in the POM phase of POM/(PS/PPE) blends

	POM/PS	POM/Ha4	POM/Ha7
Offset of $T_{c,bulk}$			
wt.% POM	50–40	50–40	15
Droplet diam. (μm)	>2.28	>1.85	≈0.5
Particles/tot area% POM (μm^{-2})	<0.18	<0.25	≈4.3
Fraction POM droplets	1	1	0.83
Particles/area% POM droplets (μm^{-2})	<0.18	<0.25	≈3.7
Volume droplets (μm^3)	>6.21	>3.32	0.065
$N_1 \gg 1/V_D$ (cm^{-3})	2×10^{11}	3×10^{11}	150×10^{11}
$N_1 \gg 1/N_D V_D$ (cm^{-3})	2×10^{11}	3×10^{11}	43×10^{11}

melt-viscosity of the amorphous matrix phase. This agrees with our SEM observations that at a constant blend composition, the fraction of co-continuous PS/PPE increases with increasing melt-viscosity of the PS/PPE phase, on account of a strongly retarded phase inversion process [1,24,25].

3.3.3. Correlation of fractionated crystallization with the blend phase morphology. Does the physical state of the matrix play a role?

Blend phase morphology is often accepted as the sole criterion for fractionated crystallization [7]. Blends in which the amount of droplets of the minor crystallizable component exceed the number of heterogeneous nuclei active at $T_{c,bulk}$, hence should display invariably fractionated crystallization. If the phase morphology is the only factor playing a role, a unique relationship between the number of droplets per volume percentage POM and the intensity of fractionated crystallizing droplets would be expected. Fig. 11 displays the relation between the quantity of fractionated crystallizing material and the most important morphological parameters such as the POM particle diameter and the number of particles per unit POM.

From Fig. 11, it is clear that only the knowledge of the blend phase morphology and the number of heterogeneous nuclei active at $T_{c,bulk}$ is not sufficient in predicting or understanding the degree of fractionated crystallization. LH blends, as for example POM/Ha7, deviate strongly from the correlation found for LL polymer blends. When considering that in the former case the number of particles per volume fraction POM consist mainly of very small subinclusions, even a more pronounced fractionated crystallization would have been expected, as the probability for smaller droplets to contain foreign heterogeneities is lower. This observation suggests that the POM phase in LH blends can make use of an additional source of heterogeneous nuclei active at $T_{c,bulk}$.

An estimation of the number of nuclei active at $T_{c,bulk}$ can be made from Fig. 11, and Eq. (3) given by Frensch et al. [7,8].

$$N_1 V_D \ll 1 \qquad \text{for fractionated crystallization.} \tag{3}$$

Eq. (3) assumes that at least 1 heterogeneity is required in each POM volume to have a bulk nucleated crystallization. An overview of the estimated nucleation density in the different POM/(PS/PPE) blends is given in Table 6.

It is indeed clear that the nucleation density, N_1, in POM/Ha7 blends has increased in comparison with both LL blends. The nucleation density in POM/PS or POM/Ha4 blends was of the order of 2×10^{11}–3×10^{11} nuclei/cm^3 and did not seem to be very sensitive to a changing matrix phase. The nucleation density in POM/Ha7 blends was found to be of the order of 0.5×10^{12} nuclei/cm^3, which implies about a ten-fold increase of the nucleation density.

Several hypothesis on the origin of these extra nuclei can be made: (i) The amorphous PS/PPE phase acts as a nucleating substrate when it has solidified before POM starts to crystallize. (ii) PPE contains a large amount of heterogeneities active at $T_{c,bulk}$, which migrate during the melt- mixing process towards the POM phase. (iii) Migration of heterogeneous nuclei during melt-mixing away from the POM phase is reduced by the high viscosity of PS/PPE compounds with a high fraction of PPE, and by the slowly developing phase morphology.

No unambiguous proof was found to support one of these three hypothesis. Hypothesis (ii) can be rejected rather easily because the slight decrease of $T_{c,bulk}$ in all blends where POM forms the matrix phase indicates a migration of impurities from the POM phase towards the PS/PPE phase. A sudden reversion of the migration direction is very unlikely, as migration is determined by the interfacial tension, $\sigma_{12,}$ which remains quasi constant in all blend systems. Remark that the depression in the onset temperature of $T_{c,bulk}$ in both POM/Ha7 and POM/Ha8 blend series is quasi similar, while it is significantly higher in the POM/Ha6 blend series. The most fundamental difference between both blend series, besides the fraction POM present as a co-continuous phase, is the fact that the onset of crystallization in POM/Ha8 and POM/Ha7 blends starts in the presence of a solidified PS/PPE matrix phase (see Fig. 1) while the PS/PPE matrix in POM/Ha6 series only starts to solidify after crystallization has started. As such, it seems reasonable to assume that the *physical state* of the amorphous PS/PPE matrix indeed influences the crystallization behavior of the finely dispersed POM particles.

The nucleating ability of POM on PS/PPE surfaces in the melt state can be estimated from the value of the spreading coefficient, F_{ij}, based on the surface tension, σ, of both components in the melt state and the interfacial tension, $\sigma_{12,}$ between POM en PS/PPE (Eq. (4)). A positive wetting coefficient indicates that the nucleation of phase i is promoted on surfaces of phase j.

$$F_{ij} = \sigma_j - \sigma_i - \sigma_{ij}. \tag{4}$$

Data on the surface tension and interfacial tension in

POM/(PS/PPE) systems have been reported by us earlier [22]. For the calculations, values for the surface tension of $\sigma_{POM}(150°C) = 53.5$ mN/m and $\sigma_{PS/PPE}(150°C) = 34$ mN/m were used. The interfacial tension between POM and PS/PPE is about 10 mN/m at 150°C. A wetting coefficient $F_{POM/(PS/PPE)}$ of −29 mN/m is calculated, indicating that PS/PPE in the melt state does not have any nucleating ability on the POM phase. An estimation of the nucleating ability of a solidified PS/PPE phase for POM could not be performed because data on the surface tension of solid PS/PPE are not available. However, it is known that the surface tension of a material suddenly increases upon solidification, which could make F_{ij} to become slightly positive.

3.3.4. When does multiple crystallization peaks occur and what determines the intensity of these subsidiary peaks?

From Figs. 6 and 7, subsidiary crystallization peaks around 127 and 114°C can be observed, besides the bulk and homogeneous crystallization exotherms. Both the blend composition range where such peaks can be observed, as the intensity of the peaks become smaller with increasing T_g of the matrix phase. Further, POM/Ha7 and POM/Ha8 blend series do not show crystallization around 127°C anymore, while in POM/Ha6 blends, the latter peak has become quasi negligible. The crystallization exotherm around 114°C could be observed in all blend series but behaves similar to the peak at 127°C; its importance is drastically reduced in the LH blends, both with respect to the peak intensity as with respect to the blend composition range where it can be observed. From the knowledge of the blend phase morphology, it can be concluded that both subsidiary crystallization exotherms should be related typically to the broadness of the POM particle size distribution in POM/PS and POM/Ha4 blends (Fig. 5(c)). POM/PS blends for example, having a broad POM particle size distribution, indeed show subsidiary crystallization peaks over a broad composition range (10–40 wt.% POM), from the point the bulk nucleation peak disappears. Klemmer and Jungnickel [5] investigated POM/HDPE blends and have attributed the exotherm around 127°C to an interface-induced additional inhomogeneous nucleation. Koutsky et al. [4] and Burns and Turnbull [47] studied the crystallization of physically dispersed droplets by optical microscopy. These authors reported that the larger droplets (6–20 μm) crystallized typically at intermediate temperatures, where crystallization occurred instantaneous at the surface of the droplets, and the crystal growth was slow. As the droplets become too small, volume limitations will start to slow down the crystallization kinetics [42]. At constant cooling rate conditions, smaller droplets hence do not crystallize anymore at these intermediate crystallization temperatures and are forced to crystallize homogeneously. The intensity of the crystallization peaks at each of the intermediate crystallization temperatures is thus correlated with the fraction of POM particles that does not contain heterogeneities active at $T_{c,bulk}$, and has dimensions to all sides that are large enough to be nucleated at the interface or by other solid impurities without suffering from a retarded crystallization kinetics due to volume limitations.

3.3.5. What causes the degree of crystallinity to decrease in fractionated crystallizing samples?

It has been demonstrated that the enthalpy of crystallization at $T_{c,bulk}$ ($\Delta H_c = -167$ J/g POM) is significantly higher than the value found in fully homogeneously crystallizing samples ($\Delta H_c = -115$ J/g POM). Applying the correction factor that takes into account the temperature dependence of the reference enthalpy function, ΔH^o, still does not level off the observed decrease in the degree of crystallinity. Attempts to find some direct relationship between the blend phase morphology and the degree of crystallinity in the POM phase mostly failed. It was expected that a more pronounced fractionated crystallization behavior, as is the case in POM/(PS/PPE) blends with lower content of POM and thus having a smaller particle size, could be directly correlated to the degree of crystallinity. However, only POM/PS and POM/Ha4 blends seem to adopt such a relationship (Fig. 12). No correlation could be found for POM/Ha7 blends.

It is indeed rather unlikely that the degree of crystallinity in the latter blend system would correlate with the average droplet size of the fraction dispersed POM. As a consequence of its composite-like morphology, subinclusions in which homogeneous crystallization results in rather low degrees of crystallinity (i.e. 40%) coexist with a co-continuous POM phase in which heterogeneous crystallization at $T_{c,bulk}$ leads to much higher degrees of crystallinity (i.e. 54%). As there is no direct relation between the dispersed POM particle size and the fraction of POM droplets, any correlation between X_c and the POM particle size should be excluded. However, as the fraction of POM droplets should reflect all homogeneously crystallized material, a correlation between both parameters indeed could be found (Fig. 13). As such, it becomes possible to estimate the fraction of

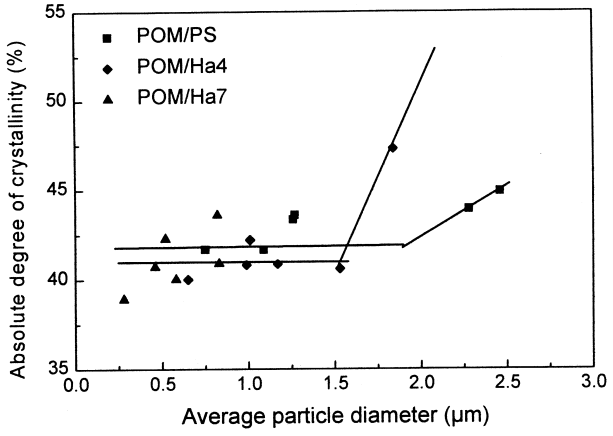

Fig. 12. Relationship between the absolute degree of crystallinity, X_c, of the POM phase and the average particle diameter of the POM droplets.

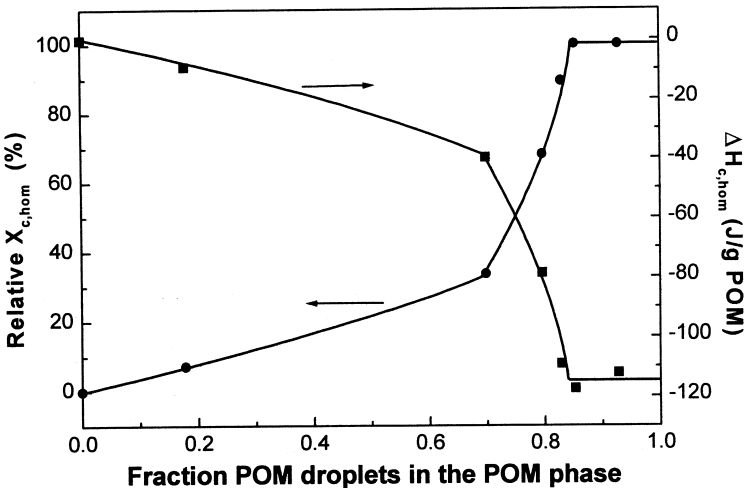

Fig. 13. Correlation between the fraction of POM droplets in POM/Ha7 blends with a composite-like phase morphology, and the intensity of the homogeneous crystallization peak.

droplets in composite-like blends, from the fraction of homogeneously crystallized material.

When considering the background of crystallinity, one should try to find causes for the decrease in X_c in the direction of the much lower crystallization temperature and/or the change in the semicrystalline morphology. Because the crystal growth rate at high degrees of undercooling is significantly higher, formation of thinner and/or less perfect lamellae can be expected. This hypothesis can be supported by the DSC melting curves, in which a shift of the melting peak to lower temperatures indeed indicates the melting of thinner or less perfect lamellar structures. However, the available information from DSC still remains interpretable. Further, other polymorphic forms (with a different crystallization enthalpy) could have grown at higher degrees of undercooling. Small Angle X-ray Scattering (SAXS) in combination with Wide Angle X-ray Diffraction (WAXD) and DSC is a powerful and unambiguous technique to gather all necessary information on the lamellar and crystalline cell structure of semicrystalline materials. A detailed investigation on this topic is discussed in the next part of this paper series.

4. Conclusions

The fractionated crystallization behavior in immiscible POM/(PS/PPE) blends has been investigated by Differential Scanning Calorimetry (DSC) and correlated to the blend phase morphology. Both the influence of the blend phase morphology and the physical state of the PS/PPE matrix on the fractionated crystallization behavior could be investigated by using PS/PPE compounds of varying PPE content. This model systems allows to alter the viscosity ratio and T_g of the matrix phase without altering the interfacial tension of the blend system.

The *blend phase morphology* in LL blends (i.e. POM/PS and POM/Ha4 blends, $p \geq 1$) was found to be very different than in LH blends (i.e. POM/Ha6, POM/Ha7 and POM/Ha8 blends, $p \ll 1$). The first group displayed a typical droplet-in-matrix phase morphology when one of the phases is in excess; a narrow region of phase inversion where the phase morphology is perfectly co-continuous is formed around a 50/50 blend composition. Blend series containing a highly viscous PS/PPE phase (LH blends) formed a very broad region of phase inversion with a complex composite like phase morphology consisting of co-continuous POM structures and fine POM subinclusions as a consequence of a non-equilibrium blend phase morphology. Outside this region, a very fine POM dispersion with a narrow particle size distribution is formed.

The *crystallization and melting behavior* in immiscible POM/(PS/PPE) blends where POM is the minor component has been investigated by DSC. Fractionated crystallization has been observed in all blend series. Four discrete crystallization temperatures of the POM phase could be observed. Bulk nucleation from heterogeneities with the lowest specific interfacial energy difference, Δy_1, is observed around 145°C. Subsidiary crystallization peaks around 127 and 114°C originating from droplets that do not contain nuclei active at $T_{c,bulk}$ and are nucleated from smaller and/or less perfect heterogeneities with a higher Δy_i, are observed mainly in the LL blends. Homogeneous crystallization by self-association of polymer chains was observed around 91°C, and is typically recognised by the extremely high conversion rates as a result of catastrophic nucleation. Within each blend series, a gradual decrease of the bulk crystallization enthalpy and increase of the homogeneous crystallization enthalpy is observed with decreasing contents of POM. The total degree of crystallinity, X_c, however was reduced significantly from 54% in fully bulk nucleated samples to about 40% in fully homogeneously crystallized samples.

A good *correlation between the blend phase morphology*

and the fractionated crystallization behavior is observed. The onset composition for fractionated crystallization could be directly related to the center of the phase inversion region for all blend series. Multiple crystallization peaks could be related to the broadness of the particle size distribution. Droplets containing no heterogeneities active at $T_{c,bulk}$ were shown to be able to nucleate at higher degrees of undercooling from an interface or other solid heterogeneities, if the droplet size was large enough not to slow down the crystallization kinetics too much as a consequence of volume limitations. Crystallization at intermediate temperatures thus occurs typically in the medium sized droplets of broad particle size distributions, as is the case in LL blends (i.e. POM/PS and POM/Ha4).

The fundamental difference between LL and LH blends in the development of the blend phase morphology during melt-mixing is reflected in different aspects of the fractionated crystallization behavior. LL blends typically show multiple crystallization peaks as soon as the bulk nucleation peak has disappeared. In LH blends, the broadened region of phase inversion with its composite droplet type morphology allows both a fraction of bulk nucleated POM, related to the amount co-continuous POM, and a fraction of homogeneously nucleated POM, related to the small subinclusions of POM in the co-continuous PS/PPE domains.

Within the same blend series, the degree of homogeneous crystallization can be related to the blend phase morphology (i.e. the number of droplets per volume percentage of the dispersed phase). However, comparing different blend series reveals that other factors, such as the physical state of the PS/PPE matrix, also play a role in LH blends; a larger portion of small POM droplets can nucleate at $T_{c,bulk}$ if the matrix has solidified before crystallization starts.

Acknowledgements

The authors are indebted to Dow Benelux N.V. (Terneuzen, The Netherlands) for the financial support of this research project. General Electric Plastics (Bergen-op-Zoom, The Netherlands) is acknowledged for supplying the PPE-800, and DSM Research (Geleen, The Netherlands) is thanked for giving us the opportunity of melt-blending the PS/PPE mixtures.

References

[1] Everaert V, Groeninckx G, Aerts L. Polymer 1999;40:6627.
[2] Utracki LA. Polymer alloys and blends, Munich: Hanser Publishers, 1989.
[3] Folkes MJ, Hope PS, editors. Polymer blends and alloys London: Blackie, 1993.
[4] Koutsky JA, Walton AG, Baer E. J Appl Phys 1967;38:1832.
[5] Klemmer N, Jungnickel BJ. Colloid Polym Sci 1984;262:381.
[6] Frensch H, Jungnickel BJ. Colloid Polym Sci 1989;267:16.
[7] Frensch H, Harnischfeger P, Jungnickel BJ. In: Utrachi L, Weiss RA, editors. Multiphase polymers: blends and ionomers, ACS Symposium Series, 395, 1989.
[8] Frensch H, Jungnickel BJ. Plastics. Rubber and Comp Processing and Appl 1991;16:5.
[9] Tang T, Huang B. J Appl Polym Sci 1994;53:355.
[10] Santana OO, Müller AJ. Polym Bull 1994;32:471.
[11] Baïltoul M, Saint-Guirons H, Xans P, Monge P. Eur Polym J 1981;17:1281.
[12] Müller AJ, Arnal ML, Morales RA. Europhysics Conference Abstracts, 19D, P2, Prague, 17–20 July 1995.
[13] Morales RA, Arnal ML, Müller AJ. Polym Bull 1995;35:379.
[14] Ghijsels A, Groesbeek N, Yip CW. Polymer 1982;23:1913.
[15] O'Malley JJ, Crystal RG, Erhardt PF. ACS Div Polym Chem, Polym Prepr 1969;10:796.
[16] Tang T, Huang B. J Polym Sci, Polym Phys Ed 1994;B32:1991.
[17] Ikkala OT, Holsti-Miettinen RM, Seppälä J. J Appl Polym Sci 1993;49:1165.
[18] Moon HS, Ryoo BK, Park JK. J Polym Sci, Polym Phys Ed 1994;B32:1427.
[19] Vonnegut BJ. J Colloid Sci 1948;3:563.
[20] Schultz AR, Gendron BM. J Appl Polym Sci 1972;16:461.
[21] Prest WM, Porter RS. J Polym Sci, Polym Phys 1972;10:1639.
[22] Everaert V, Groeninckx G, Aerts L, Pionteck J, Favis B, Moldenaers P, Mewis J. Polymer 1999; in press.
[23] Scott CE, Joung SK. Proceedings of the SPE Retec Symposium on Polymer Alloys and Blends, Boucherville, Canada, October, 1995, p. 338.
[24] Sundararaj U, Macosko CW, Shih CK. Polym Engng Sci 1996;36:1769.
[25] Sundararaj U. Macromol Symp 1996;112:85.
[26] Elmendorp JJ. In: Rauwendaal C, editor. Mixing in polymer processing, New York: Marcel Dekker, 1991.
[27] Fortelný I, Zivný A. Polymer 1995;36:4113.
[28] Jackson KA. Ind Engng Chem 1965;57:29.
[29] Hoffman JD, Weeks JJ. J Chem Phys 1962;37:1723.
[30] Barham PJ, Jarvis DA, Keller A. J Polym Sci, Polym Phys Ed 1982;20:1733.
[31] Macromolecular physics. In: Wunderlich BB, editor. Crystal nucleation, growth, annealing, 2. New York: Academic Press, 1976.
[32] The ATHAS Data Bank, Wunderlich BB, editor. Available on www.
[33] Gaur U, Wunderlich B. J Phys Chem Ref Data 1981;10:1001.
[34] Suzuki H, Wunderlich B. J Polym Sci, Polym Phys Ed 1985;23:1671.
[35] Blais JJ, Manley R. J Macromol Sci 1967;B1:525.
[36] Peeters M. PhD Thesis, KULeuven, Belgium, 1995.
[37] Everaert V, Groeninckx G, Koch MHJ, Reynaers HR. Submitted for publication to Macromolecules, 1999.
[38] Quintens D, Groeninckx G, Guest M, Aerts L. Polym Eng Sci 1990;30:1474.
[39] Galeski A, Bartczak Z, Pracella M. Polymer 1984;25:1323.
[40] Bartczak Z, Galeski A, Pracella M. Polymer 1986;27:537.
[41] Bartczak Z, Galeski A, Krasnikova NP. Polymer 1987;28:1627.
[42] Billon N, Chanial L, Vivien B, Haudin JM. Ann Chim Fr 1995;20:355.
[43] Escleine JM, Monasse B, Wey E, Haudin JM. Colloid Polym Sci 1984;262:306.
[44] Billon N, Haudin JM. Colloid Polym Sci 1989;267:1064.
[45] Billon N, Haudin JM. Ann Chim Fr 1990;15:173.
[46] Avrami M. J Chem Phys 1940;8:212.
[47] Burns JR, Turnbull D. J Appl Phys 1966;37:4021.
[48] Groeninckx G, Vanneste M, Everaert V. Crystallization, morphological structure and melting behavior in polymer blends. In: Utracki LA, editor. Polymer blends handbook, Dordrecht: Kluwer Academic Publishers, 1999 in press.